Injection-Molded High-Density Polyethylene–Hydroxyapatite–Aluminum Oxide Hybrid Composites for Hard-Tissue Replacement: Mechanical, Biological, and Protein Adsorption Behavior

Garima Tripathi, Bikramjit Basu*

Laboratory for Biomaterials, Department of Material Science and Engineering, Indian Institute of Technology, Kanpur 208016, Uttar Pradesh, India

Received 4 May 2011; accepted 8 July 2011
DOI 10.1002/app.35236
Published online 26 October 2011 in Wiley Online Library (wileyonlinelibrary.com).

ABSTRACT: In this article, we report the mechanical and biocompatibility properties of injection-molded high-density polyethylene (HDPE) composites reinforced with 40 wt % ceramic filler [hydroxyapatite (HA) and/or Al_2O_3] and 2 wt % titanate as a coupling agent. The mechanical property measurements revealed that a combination of a maximum tensile strength of 18.7 MPa and a maximum tensile modulus of about 855 MPa could be achieved with the injection-molded HDPE–20 wt % HA–20 wt % Al_2O_3 composites. For the same composite composition, the maximum compression strength was determined to be 71.6 MPa and the compression modulus was about 660 MPa. The fractrography study revealed the uniform distribution of ceramic fillers in the semicrystalline HDPE matrix. The cytocompatibility study with osteoblast-like SaOS2 cells confirmed extensive cell adhesion and proliferation on the injection-molded HDPE–20 wt % HA–20 wt % Al_2O_3 composites. The cell viability analysis with the 3(4,5-dimethylthiazol-2-yl)-2,5-diphenyltetrazolium bromide assay revealed a statistically significant difference between the injection-molded HDPE–20 wt % HA–20 wt % Al_2O_3 composites and sintered HA for various culture durations of upto 7 days. The difference in cytocompatibility properties among the biocomposites is explained in terms of the difference in the protein absorption behavior. © 2011 Wiley Periodicals, Inc. J Appl Polym Sci 124: 2133–2143, 2012

Key words: biocompatibility; injection molding; mechanical properties

INTRODUCTION

In terms of compositional aspect, bone tissue is considered as a complex hybrid composite material that is composed of collagen fibrils (polymer matrix) and hydroxyapatite (HA) crystals (inorganic reinforcement). The mechanical response of human bone is related to mineralization and anatomical location.[1,2] For hard-tissue replacement materials, their mechanical behavior needs to be critically considered, as the stiffness of the implant determines the load sharing between the implant and the surrounding tissue.[3–5] Therefore, the bone-matching mechanical performance is the critical issue to ensure the positive mechanical response of the implant.

In last few decades, attention has been directed towards the development of polymer–ceramic composites for load-bearing orthopedic applications. The main advantage of the use of such composites is the fact that by varying the type and amount of the reinforcing phase, one can tailor their mechanical and biological properties for desired applications.[6] Polymer–ceramic composites, with tailored modulus and strength values, provide advantages compared to pure polymers, ceramics, and metals for hard-tissue replacement applications.

Attempts to enhance the mechanical performance of thermoplastic polymers [e.g., high-density polyethylene (HDPE)] to allow for their use as hard-tissue substitutes have partially relied on the use of HA reinforcement. HA, with the molecular stoichiometric formula $Ca_{10}(PO_4)_6(OH)_2$, has attracted wider attention because of its excellent biocompatibility, bioactivity, and osteoconductivity properties. However, its poor compressive strength and toughness limits its applicability to low-load- or non-load-bearing applications in the human body.[7] Extensive research has been carried out to develop HA-based composite materials, and a variety of polymers have been used. The bone-analogue concept, which proposes composites of a ductile polymer matrix

**Present address:* Laboratory for Biomaterials, Materials Research Centre, Indian Institute of Science, Bangalore 560012, India.

Correspondence to: B. Basu (bikram@iitk.ac.in).

Contract grant sponsor: Department of Science and Technology, New Delhi, India (under the Fast Track Young Scientist Scheme).

[polyethylene (PE)] and a stiff ceramic phase (HA), was initially proposed by Bonfield and coworkers.[8–15] However, the lower strength, modulus, and stiffness of these composites compared to cortical bone have limited their application as load-bearing bone substitutes. Reis et al.[16] provided an alternative approach to enhance the mechanical performance of fabricated HDPE/HA composites using shear controlled orientation in injection molding. Also, Pandey et al.[17] reported that HDPE–HA composites could exhibit an elastic modulus of 206–531 MPa, strengths in the range 20–24.3 MPa, and elongations at break of 8.3–163%. Recently, the injection molding of middle-ear implants with HA–HDPE composition was carried out successfully.[18]

A review of the literature revealed that the mechanical properties of polymer–ceramic composites critically depend on interfacial bonding between the reinforced material and the matrix.[19,20] The adhesion of the reinforcement to the matrix can have a significant effect on the characteristics and properties of the composites.[21] PE is a nonpolar, hydrophobic polymer, and consequently, mechanical interlocking exists between the HA particles and the PE matrix in a conventionally processed HA–HDPE composite.[22] The chemical interaction between the filler and the polymer will lead to much improved bonding and, hence, mechanical properties.[8] The addition of coupling agents provides other beneficial effects and improves composite blending and injection molding. Material interaction through polar coupling and hydrogen bonding also provides good adhesion between the ceramic and polymer components.

In recent research by Nath et al.,[23] an HDPE–HA composite with Al_2O_3 reinforcement was investigated for biomedical applications. The bioinert characteristics of Al_2O_3 make it useful as a component in a great number of dental and orthopedic applications. The latest investigation of HDPE–HA–Al_2O_3 composites without any coupling agent was carried out with an injection-molding route.[24] A maximum strength of 20 MPa and a modulus of 1 GPa with a 30 vol % ceramic loading were reported. An important conclusion was that the injection molding of HDPE composites with more than 30 vol % ceramic loading was difficult because of a significant increase in the viscosity and a decrease in the flow rate. No biocompatibility study was conducted in that study.

Inspired by the previous research work, we carried out preliminary studies of chemically coupled HDPE–HA–Al_2O_3 composites using the compression-molding technique.[25] The objective was to enhance the interfacial bonding between the polymer and ceramic phases with coupling agents to promote molecular bonding and, consequently to improve interfacial adhesion.[26,27]

Carrying this work forward, we decided to use the injection-molding route so that the ability to make complex-shaped materials from the HDPE–HA–Al_2O_3 compositions could be assessed. This was in view of the fact that an important advantage of injection molding is that the processed material can be easily shaped into complex geometries in a short production cycle or in a single run; this improves the mechanical properties and microstructure.

In this article, we report the systematic investigation of the role of the polymer, ceramic, and coupling agent on the injection molding of HDPE–HA–Al_2O_3 hybrid biocomposites. The objective of this work was to analyze the physicomechanical behavior and biocompatibility of the composites. We also evaluated the cell adhesion, cell viability, and protein absorption in a systematic manner. All the obtained data were critically analyzed to assess the suitability of the injection-molded HDPE–HA–Al_2O_3 composites for bone-replacement applications.

EXPERIMENTAL

Starting material

In this research, commercially available HDPE was used as the matrix, and it was procured from Swasan Chemicals (Mumbai, India). Both HA and Al_2O_3 were used as reinforcements. HA was synthesized by the widely reported suspension–precipitation route, as described in our earlier work.[28] The precursor materials were CaO (M/S S. D. Fine-Chem, Ltd., product number 37614), H_3PO_4 (M/S Merck, Chemical Abstracts Service number 7664-38-2), and NH_4OH (M/S Qualikems, product number A025112). Besides HA, commercially available alumina (α-Al_2O_3, average size = 4.8 μm, 99.4% pure, Carborumdum Universal, Chennai, India) was used as another ceramic filler in the composites. The coupling agent used in this study was titanium IV 2-propanolatotrisisooctadecanoato-O, obtained from Kenrich Chemicals Pvt., Ltd, Bayonne, NJ, USA.

At the start, HDPE, HA, and Al_2O_3 were physically mixed in the presence of 2 wt % coupling agent. In view of our earlier research on the HDPE–HA–Al_2O_3 system,[25] it was decided to load 40 wt % filler (20 wt % HA and 20 wt % Al_2O_3) in polymer matrix. Injection molding was carried out at a barrel temperature of 180°C and a mold temperature of 25°C. The available cooling time was 30 s. The process was followed with a back pressure of about 3 MPa.

In this study, four different polymer–ceramic compositions were formulated, as shown in Table I. Unreinforced HDPE is designated as sample IS1. HA powders of 40 wt % were mixed with the HDPE matrix and the coupling agent to produce sample IS2,

TABLE I
Summary of the Data from the Mechanical Tests Performed on the Injection-Molded Samples

Sample	Designation	Composition	Densification (%)	Compressive strength (MPa)	Compressive modulus (MPa)	Tensile strength (MPa)	Tensile modulus (MPa)	Elongation at break (%)
1	IS1	HDPE	99.0	57.2 ± 1.4	469.1 ± 150.0	24.2 ± 0.9	564.3 ± 130.2	855.4
2	IS2	HDPE + 40 wt % HA (2% coupling agent)	93.4	67.0 ± 1.2	532.1 ± 148.8	14.3 ± 0.1	679.1 ± 110.4	47.9
3	IS3	HDPE + 40 wt % Al_2O_3 (2% coupling agent)	95.1	71.6 ± 1.0	312.7 ± 108.2	16.4 ± 0.8	673.4 ± 102.7	95.0
4	IS4	HDPE + 20 wt % HA + 20 wt % Al_2O_3 (2% coupling agent)	95.6	70.2 ± 1.7	660.9 ± 118.0	18.7 ± 0.4	855.4 ± 108.4	6.8

and IS3 was composed of 40 wt % Al_2O_3 with the coupling agent. The composition made from the simultaneous addition [40 wt % filler] of both HA and Al_2O_3 (1 : 1) in the presence of the coupling agent to 60 wt % HDPE powder was designated as IS4. In the IS2, IS3, and IS4 composites, 2 wt % coupling agent was used.

Physicomechanical and structural morphology characterization

The density measurement of HDPE (IS1) was carried out in alcohol and that of the other composites was carried out in water with the use of Archimedes's principle. The hardness of the developed composites was measured with a Vickers microhardness tester (Michigan City, IN, USA) with an indent load of 10 g. The tensile testing of the prepared samples was carried out with an Instron 1195 instrument (Grove City, PA, USA) at a crosshead speed of 0.5 mm/min. For all the runs, a fixed gauge length of 25 mm was used. With the help of stress–strain response, we calculated the tensile modulus and percentage elongation at break. Compression tests were also performed on the Instron 1195. The samples used for the compression test were cylinder-shaped and were tested at a crosshead speed of 0.5 mm/min with a load cell of 2 kN.

All mechanical tests were repeated three times (four specimens each time) for each material composition. Statistical analysis was performed with the statistical significance at $p < 0.05$.

In vitro biocompatibility properties

Cell culture experiments

Human osteoblast SaOS2 cells (ATCC) were revived before they were seeded on the samples. SaOS2 cells were cultured in McCoy's medium 5A (Sigma Aldrich, St. Louis, MO, USA) supplemented with 15% fetal bovine serum (FBS) and 1% penicillin/streptomycin solution. The cell lines in the sterile tissue culture flask were incubated for further proliferation and growth in a standard CO_2 incubator (Thermo, Hudson, New Hampshire, USA) operated under conditions of 5% CO_2, 95% relative humidity, and a 37°C temperature until confluent. The medium was replaced from time to time to control the pH. The confluent monolayer was detached from the tissue culture flask with 0.50% trypsin and a 0.20% ethylene diamine tetraacetic acid solution (Sigma Aldrich).

Cell adhesion test

For seeding on the composites, the prepared composites were ultrasonically cleaned, autoclaved, and then dehydrated with 70% ethanol for 24 h to sterilize them. We removed ethanol by washing the samples twice with phosphate buffer saline (PBS). The samples were then exposed to UV light for 2 h and, finally, soaked in medium containing 10% FBS for 12 h. As described in the previous subsection, SaOS2 cells were grown in McCoy's medium 5A supplemented with 10% FBS and 1% penicillin/streptomycin solution. All the samples were sterilized, and subsequently, the cells were seeded on the samples at an approximate density of 3×10^5 cells/mL using a hemocytometer. The culture plates (with four wells) and the test samples were then incubated in a CO_2 incubator in the previously described environment. The culture medium was aspirated from time to time, and fresh culture medium was added to the culture plate wells. After the stipulated time period (2–3 days), the samples were washed twice with PBS, and then, the cells were fixed with 1.5% glutaraldehyde diluted in PBS. The composition of PBS included 137 m*M* sodium chloride, 2.7 m*M* potassium chloride, 10 m*M* disodium hydrogen phosphate, and 2 m*M* potassium dihydrogen phosphate. The cells, adhered on the material surfaces, were dehydrated with a series of ethanol solutions (30, 50, 70, 90, and 100%) for 10 min twice and then further dried with hexamethyldisilazane. The dried samples

were sputter-coated (Vacuum Tech, Bangalore, India) with gold and examined with a scanning electron microscope (Philips, Quanta, Hillsboro, Oregon, USA).

3(4,5-Dimethylthiazol-2-yl)-2–5-diphenyltetrazolium bromide (MTT) assay

The MTT assay (Sigma, St. Louis, MO, USA) is a colorimetric assay that has been used to test cytotoxicity and cell viability. To perform this assay on our composites, SaOS2 cells were cultured with the previously described cell-culturing method. The sterile injection-molded composites were placed in a 24-well plate (exposed to UV light for 30 min), and the cells were seeded (200 μL McCoy's medium 5A with cell suspension, serum, and antibiotic) at an approximate density of 3×10^5 cells/mL. Subsequently, the culture plates, having replicates of each composition, were incubated for 3, 5, and 7 days in a CO_2 incubator. After the incubation periods, the medium was aspirated, and samples were washed twice with PBS. Fresh DMEM (100 μL, without phenol red) was added. In the next step, 10 μL of reconstituted MTT (Sigma) was added to each well (5 mg/mL in dulbuco's modified eagle medium, (DMEM) (Sigma Aldrich, St. Louis, MO, USA) without phenol red and serum), and each plate was incubated for 6–8 h. The culture plate was observed under a phase-contrast microscope (Nikon, Eclipse 80i, Tokyo, Japan) to check for the formation of purple formazane crystals. After the required incubation time, the samples were removed from the well, and 100 μL of dimethyl sulfoxide (stop solution) was added to each well, including the control. The optical density of the solution was measured at 540 nm with an enzyme linked immunosorbent assay (ELISA) automated microplate reader (Bio-Tek, ELx800, Winooski, Vermont, USA).

Protein absorption

The protein adsorption study was performed with a standard protein adsorption protocol [microbicinchronic acid (BCA) kit, Sigma Aldrich). The equal protein source (initial concentration ≈ 5 mg/mL) was filled in a 24-well plate containing injection-molded samples. The plate was then placed in a sterile incubator at 37°C for the standard incubation time. The samples were then washed with equal volumes of purified (deionized, DI) water to remove the nonadherent proteins. Then, all of the samples were washed with an equal amount of 1× PBS to dissolve the absorbed protein. Thereafter, 1× PBS was placed in another well plate. A 1% sodium docedyl sulfate solution was added to each well, and the wells were incubated at 50°C for 15 min. The protein concentration was analyzed with the BCA protein assay.

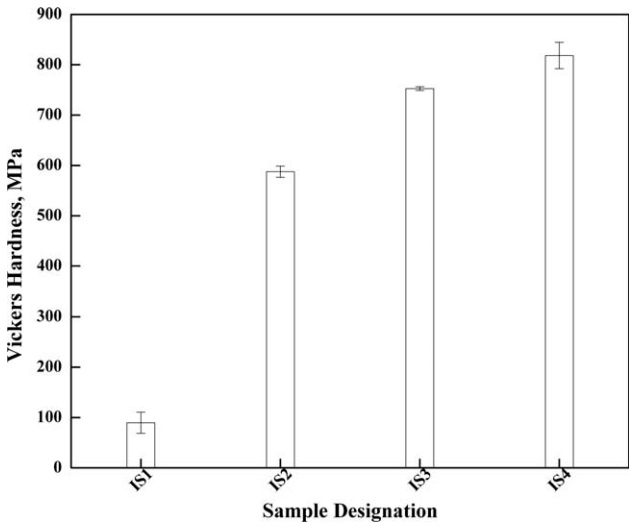

Figure 1 Vickers hardness of the prepared compositions.

In this assay, the reduction of Cu^{2+} to Cu^{1+} takes place by protein in an alkaline medium with the selective colorimetric detection of the cuprous cation (Cu^{1+}) by bicinchoninic acid. Protein reacts to produce the light blue to violet complex that absorbs light at 540 nm. Such a color change can be measured at any wavelength between 540 and 570 nm with a minimal (<10%) loss of signal. The rate of BCA color formation is dependent on the incubation temperature, the type of protein absorbed on the sample, and the relative amount of reactive amino acids contained in the proteins.

Statistical analysis

MTT analysis results were statistically analyzed with the commercial SPSS-13.0 software, New York, USA. To measure the statistical difference among the absorbance values of the prepared samples, we used the analysis of variance method. In particular, the *post hoc* comparison of the mean of independent groups were made with the Tukey test at a statistical significance value of $p < 0.05$.

RESULTS AND DISCUSSION

Physicomechanical characterization and structural morphology

In this investigation, large square discs of 80 × 80 mm^2 in size with a thickness of around 3–4 mm were obtained with both the HDPE monolith and the composites. In particular, pure HDPE processed through injection molding showed a maximum consolidation of 99% ρ_{th} (Theoretical Density), whereas the other compositions possessed densities varying in the range of 94–95% ρ_{th} (Theoretical Density). The

selected injection-molding conditions, therefore, were capable of producing rather dense composites in the HDPE–HA–Al_2O_3 system.

The indication of relative microscale deformability for polymers can be assessed with Vickers hardness testing. In Vickers hardness testing, the resistance of a material to undergo viscoelastic deformation for a polymer is typically measured under an indentation load. The obtained results for this study, as shown in Figure 1, clearly indicate that the hardness increased with the addition of 40 wt % HA in HDPE (IS2) and was found as 587 MPa, which was lower than that of the HDPE composite with 40 wt % addition of Al_2O_3 as a filler (IS3). The hardness value of IS2 increased six times compared to that of IS1. For composition IS4, that is, the composite with equal weight percentage additions of both inorganic fillers (HA and Al_2O_3), the hardness reached 818.2 MPa; this showed a ninefold increase over pure HDPE. The obtained values were in the range of hardness of human cortical bone, which ranges between 234 and 760 MPa.[21] The increased resistance to indentation of the HDPE composite could be ascribed to the relatively uniform distribution of HA and Al_2O_3 particles and the decrease in interparticle distance with particle loading in the matrix, as discussed later. We concluded that the ceramic fillers were homogeneously distributed in the polymer matrix and that the presence of the coupling agent provided better interfacial bonding between both the inorganic and organic phases.

It is well known that most polymers, when loaded, have a distinctive index for undergoing viscoelastic deformation. This type of deformation is enhanced at indent contacts in the presence of complex stress conditions. In this study, the indent impressions were not distinct; this indicated the softness of the thermoplastic phase and a significant recovery due to the viscoelastic nature. However, the prepared composites IS2, IS3, and IS4 provided higher hardness values than those reported earlier.[29–31]

The mechanical behavior of the prepared hybrid composites (IS2–IS4) were investigated by means of uniaxial tensile testing of dog-bone-shaped samples and compression testing of cylindrical-shaped samples. For comparative study, pure HDPE was also tested under identical testing conditions. The compression modulus and strength were obtained from stress versus strain response. The elastic modulus, tensile strength, and elongation at break were calculated with tensile test data. All of the experimental data are summarized in Table I.

Typical tensile stress–strain curves for various investigated materials are shown in Figure 2(a,b). The tensile modulus and elongation at break are summarized in Figure 2. The tensile modulus of the IS4 was about 1.5 times greater than that of IS1. The

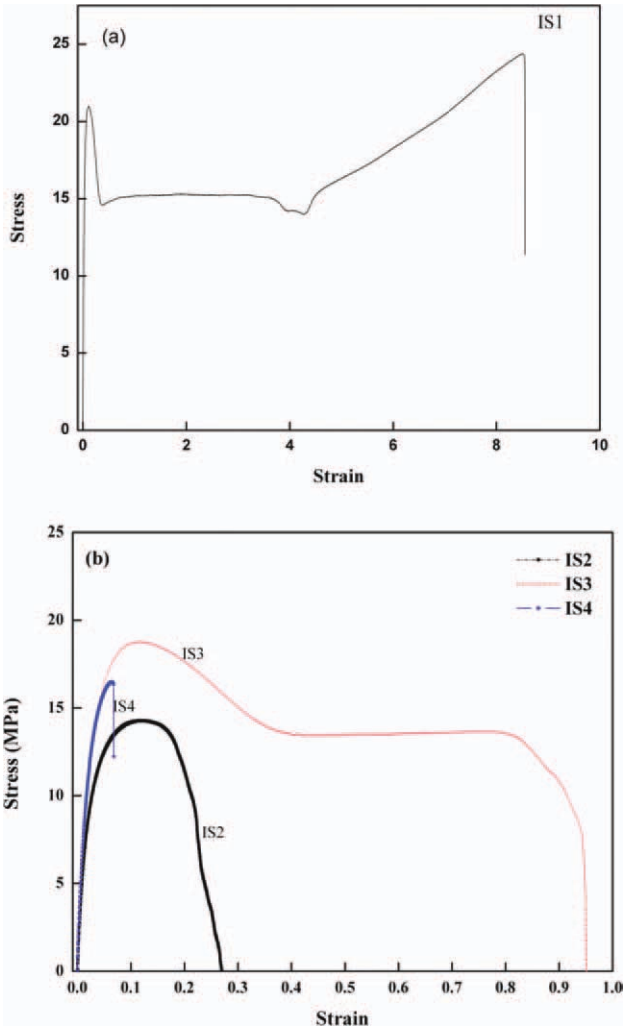

Figure 2 Typical tensile stress–strain curves of prepared composites (a) IS1 and (b) IS2, IS3 and IS4 calculated from the load-extension data of the tensile tests. [Color figure can be viewed in the online issue, which is available at wileyonlinelibrary.com.]

compressive moduli were calculated from the compressive test data, as shown in Figure 3(a,b), for IS1 and IS4. To show reproducibility in the compression behavior, the data from multiple test runs are plotted in Figure 3.

As mentioned previously, tensile tests were performed on tensile specimens of the IS1–IS4 composites. Four specimens from each set were tested, and the average for each set of specimens is plotted as a function of composition in Figure 4. The elastic modulus was calculated from the slope of the initial linear part of the stress–strain diagrams (Figs. 2 and 3). The average elastic moduli for each set of samples were also plotted as a function of their compositions (Fig. 4). The results showed that IS1 had a tensile strength of 24.2 MPa (±0.9 MPa), whereas the tensile strengths of IS2–IS4 were found to be 14.3 MPa (±0.1 MPa), 16.4 MPa (±0.8 MPa), and 18.7 MPa

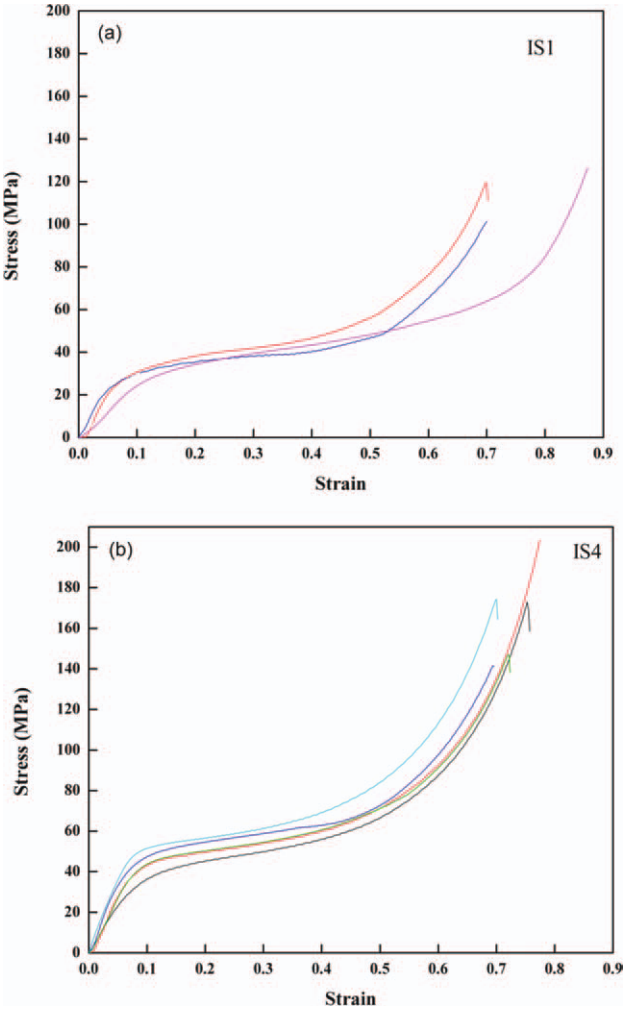

Figure 3 Typical compression stress–strain curves of (a) IS1and (b) IS4 calculated from the load-extension data of the compression tests. To illustrate the reproducibility in compression behavior, the data of multiple runs are plotted. [Color figure can be viewed in the online issue, which is available at wileyonlinelibrary.com.]

(±0.4 MPa), respectively. The tensile modulus of neat HDPE (IS1) was found to be the minimum, that is, 564.3 MPa (±130.2 MPa). It was clear from the results that the presence of the filler and coupling agent increased the tensile modulus but decreased the strength. The ceramic fillers reduced the melt viscosity and increased the plasticity of the overall composition. The IS4 composite showed highest tensile strength in comparison to IS2 and IS3 with a high tensile modulus. The presence of ceramic filler clearly increased the stiffness of the composite with no significant effect on the tensile properties. A small drop in the tensile strength for the composite samples is believed to have been due to interfacial bonding between the HDPE matrix and HA/Al_2O_3 reinforcement.

Uniaxial compression tests were carried out on four cylindrical samples for each set of as-processed composites. The ultimate compressive failure strength, compressive modulus, and compressive strength at which failure initiated in each sample were calculated from the stress–strain plot obtained for each sample. The averages of each strength value are reported and plotted in Figure 4. The compressive modulus of the IS4 composite was also about 1.5 times greater than that of IS1, that is, pure HDPE. A general observation was found in the strength of composite IS3. The presence of Al_2O_3 as a filler provided better strength to the IS3 composite compared to IS2. Another important thing that was noticed was the elastic modulus (*E*- modulus) of the composite, which could be easily correlated with the modulus of HA and Al_2O_3. The *E* moduli of HA and Al_2O_3 were about 85 and 390 GPa, respectively.[22] The maximum elongation was found in IS1 (pure HDPE), and the minimum was measured in IS3, the composite having 40 wt % Al_2O_3 (Table I).

Scanning electron microscopy (SEM) micrographs of the tensile fractured surfaces for IS1–IS4 are shown in Figure 5. For all the composites, the polymer matrix underwent extensive deformation, and long polymer flaps or wavy ligaments were observed. At higher magnification [Fig. 5(e,f)], it was observed that the HA and Al_2O_3 particles were held at the center of rings on the fractured surfaces and were still being attached to the drawn polymer matrix. This clearly suggested a strong bond between the ceramic filler and the polymer matrix, which possibly was facilitated in the presence of the coupling agent. It has been already reported that coupling agents improve the dispersion and bonding of ceramic fillers in the polymer matrix.[32,33]

In vitro biocompatibility properties

The biological performance of the injection-molded polymer–ceramic composites was evaluated with

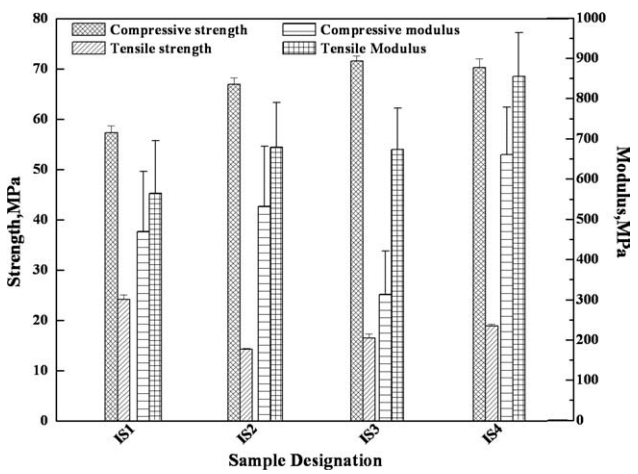

Figure 4 Comparative representation of the obtained mechanical strength and relative *E* modulus values of the prepared composites.

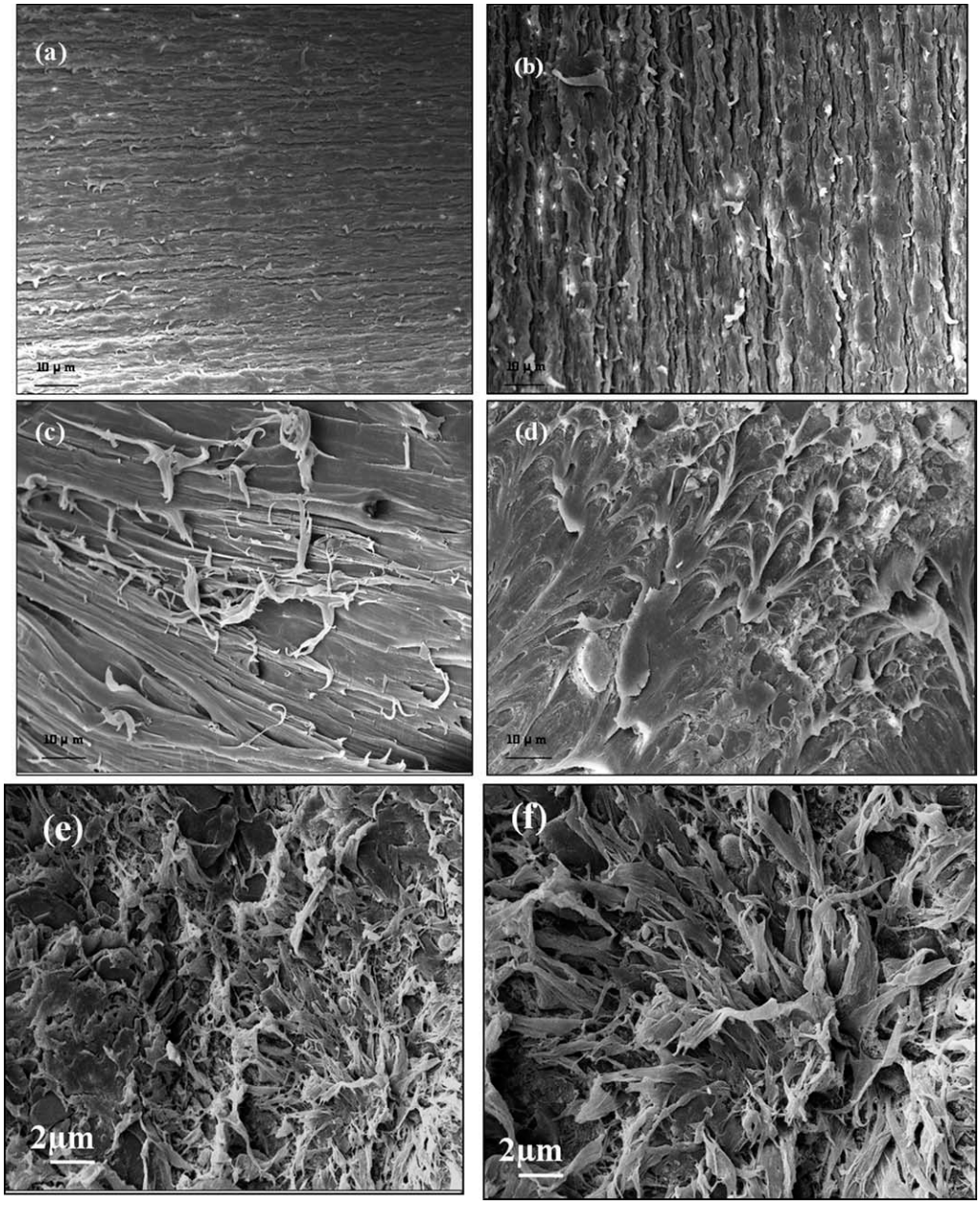

Figure 5 SEM images of the fractured surfaces obtained after tensile testing at a crosshead speed of 0.5 mm/min: (a) IS1, (b) IS2, (c) IS3, and (d) IS4. (e,f) SEM images of the fractured surfaces of IS4 after tensile testing.

SaOS2 osteoblast-like cells. SEM results indicate that the composite surfaces allowed the attachment and spreading of the cells, which kept a normal cellular morphology. After 3 days of culturing, the osteoblast-like cells reached the confluency level on the surfaces of all the compositions. Most of the cells were flattened, some were star-shaped or polygon-shaped and spread on the surface to give the similitude of cellular junctions [Fig. 6(a,b)]. The highly extended fillipodia and rough surfaces of the cells were characteristic of active cells, as shown in Figure 6(b). SEM images at higher magnification revealed the formation of an extracellular matrix, an extensive network of fibrillar and globular substances [Fig. 6(b,c)] organized and secreted by the SaOS2 cells.

To assess the cellular viability with the MTT assay, SaOS2 cells were cultured on the prepared polymer–ceramic composites for various timeframes. The osteoblast-like cell viability was found to increase in the prepared samples from day 3 to day 7 (see Fig. 7). As indicated in Figure 7, the osteoblast viability was quite similar on HA and IS4 on day 7. Similar observations were made for IS2 and HA on day 5. Although the number of viable cells on the surface of the samples, along with the control and HA disc, was significantly smaller on day 3

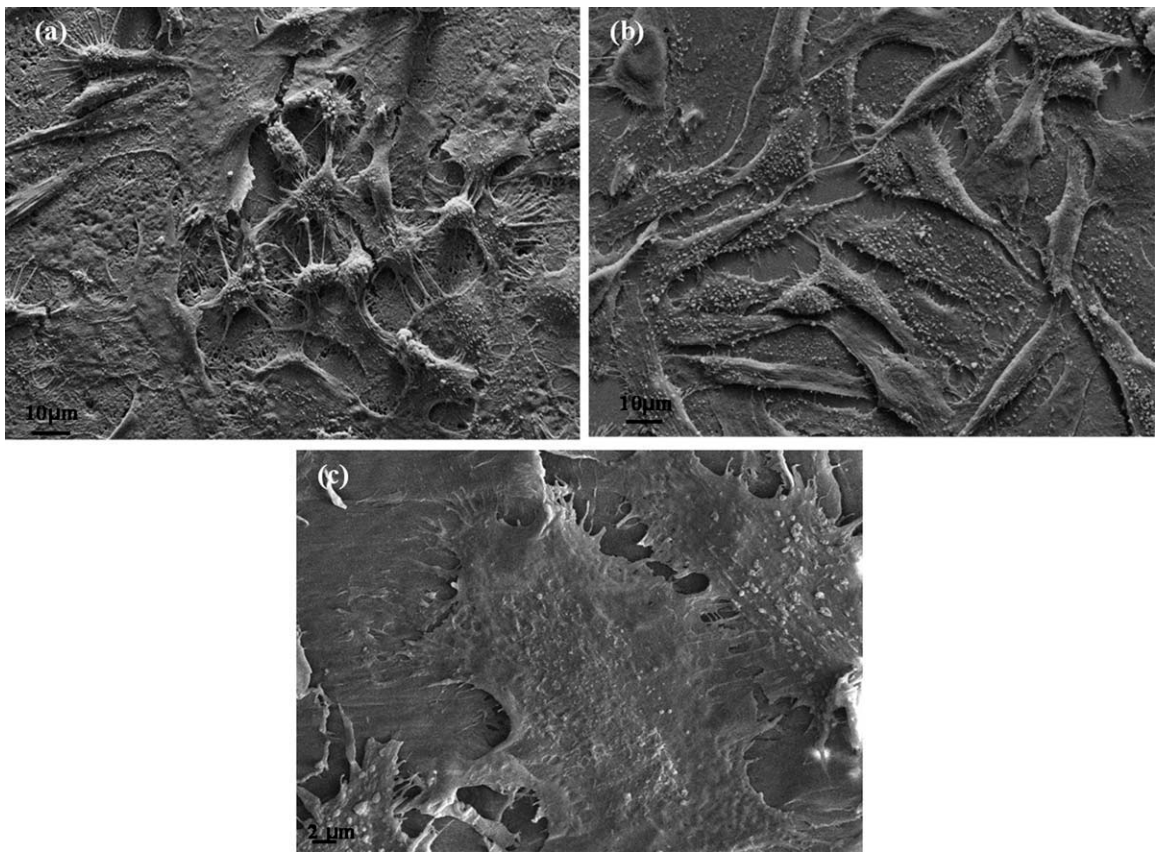

Figure 6 SEM micrographs of the osteoblast cells on the (a) composite, (b) IS2, and (c) IS4.

($p < 0.05$), there was no significant difference between the control and HA. However, the IS2, IS3, and IS4 composites were significantly different from each other. In contrast, a statistically significant increase in the cell viability was measured for the SaOS2 cells on IS4 for all 3, 5, and 7 days of culturing ($p < 0.05$).

In the investigated HDPE–HA–Al_2O_3 composites, significant differences in the osteoblast adhesion and spreading on the surface depended on the differences in chemical composition and topography of the substrates.[34–37] To show the surface topographical features of the investigated composites, Figure 8 presents some representative high-magnification SEM images of the composites. A closer look at Figure 8(a–c) reveals more rough surface features in the IS4 composite as compared to the IS3 composite. The IS2 composite surface also appeared to be rougher than that of the IS3 composite. The presence of unevenness, cracks, and pores contributed to the surface roughness. The presence of pores and a rough surface [Fig. 8(a,c)] was reflected in higher protein adsorption and cell growth. The cell adhesion behavior, cell viability, and protein adsorption behavior were more enhanced in the IS4 composite compared to the IS3 composite. In this investigation, IS2 and IS4 showed better cell viability than IS3. Despite the initial delay in cell proliferation on IS4, SaOS2 cells, nevertheless, appeared to proliferate significantly with longer culture duration. IS3 showed less proliferation in all the days of culture. This

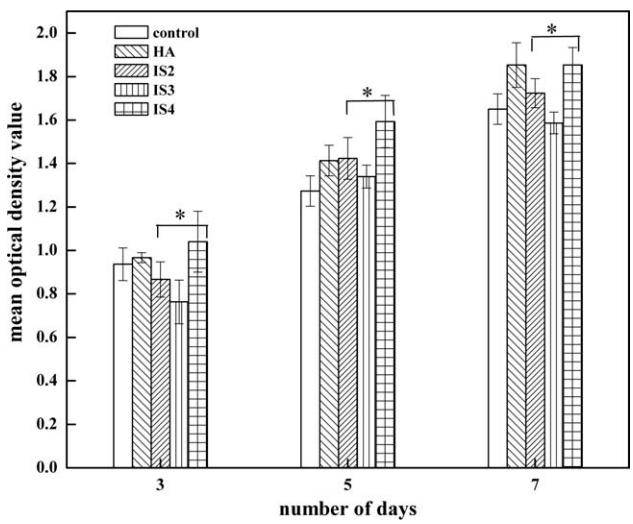

Figure 7 MTT assay results showing the SaOS2 cells on the control, HA, and composite samples after 3, 5, and 7 days of culturing. An asterisk represents a significant difference at $p < 0.05$ with respect to the compositions, and the error bars correspond to ±1.00 standard error for the number of days of culturing. OD, optical density.

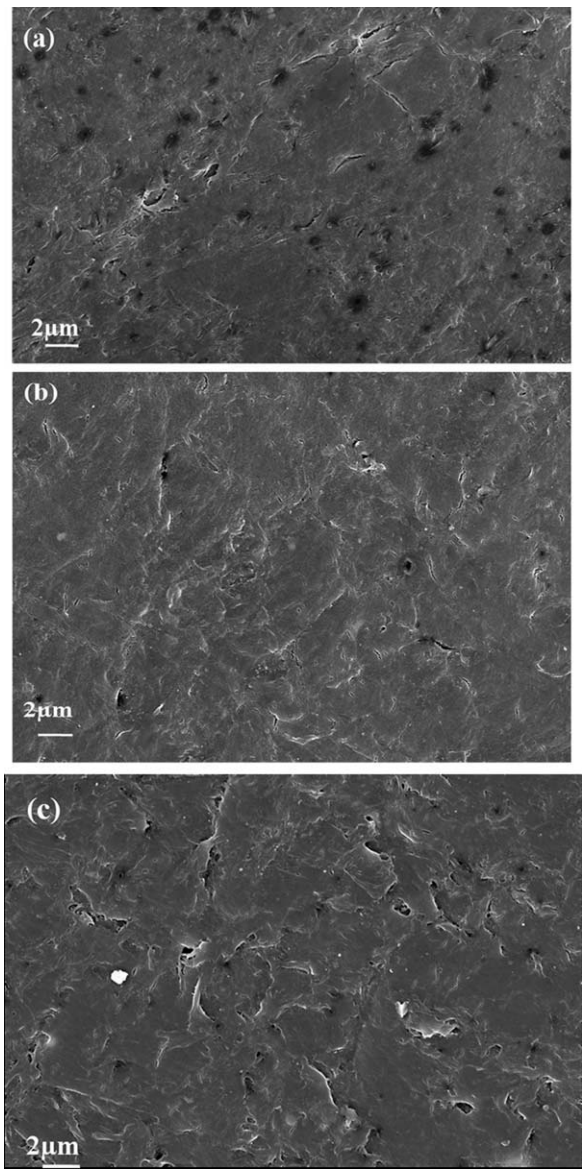

Figure 8 Higher magnification images of the samples showing the surface morphologies: (a) IS2, (b) IS3, and (c) IS4.

could be correlated with the better biocompatibility of HA compared to Al_2O_3.

The difference in cell viability or cell proliferation among the IS1–IS4 materials could be better explained in terms of differences in the protein absorption behavior. Proteins are amphiphatic molecules, which typically adhere to the surface of a biomaterial in a non-specific manner. In different cases, such non-specific adhesion is sufficient to artificially immobilize proteins on the material surface, and no surface modification is necessary. The high hydrophobicity of many proteins has been reported to play an important role in their absorption on particle surfaces.[38] In this study, bovine serum albumin, a soft protein, was used. Soft proteins are reported to be able to change their conformation better than hard proteins. When absorbed on solid surfaces, soft proteins improve the efficacy of the absorption process compared to hard proteins, such as fibrinogen, α-chymotrypsin, ribonuclease, lysozyme, and β-lactoglobulin.

The protein absorption behavior of biomaterials is dependent on the presence of biocompatible phases in the composite surface. In this case, the maximum absorption was measured for HA, IS2, and IS4, as shown in Figure 8(a). This might have been due to the presence and homogeneous distribution of the biocompatible HA filler. For example, a lower absorption was noticed in IS3; this was further reflected in the cell viability measured by the MTT assay. This might have been correlated with the presence of Al_2O_3, which was comparatively less biocompatible than HA. The protein absorption behavior of the prepared composites showed statistically significant differences among IS2, IS3, and IS4 with respect to HA and the control disc (Fig. 9).

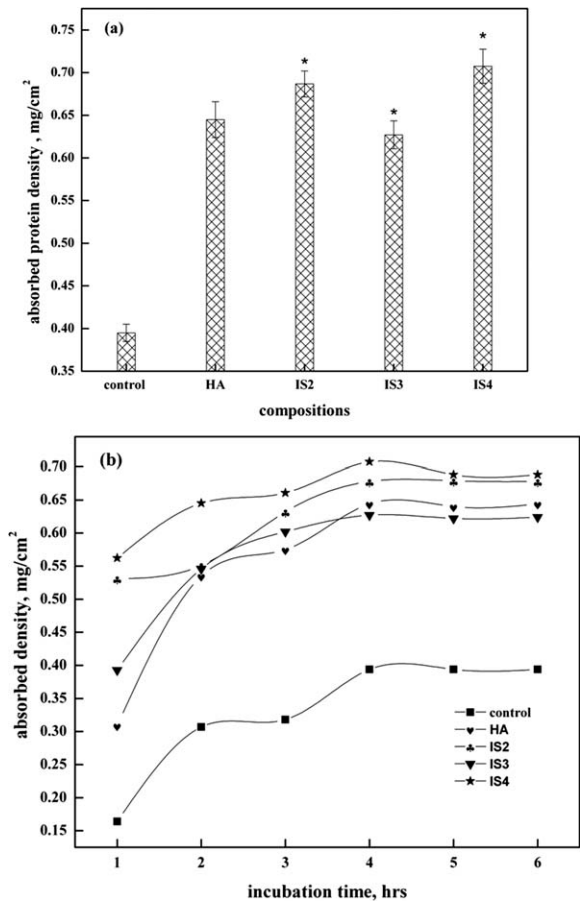

Figure 9 Protein absorption of the composites: (a) composition versus absorbed protein density (incubation time = 4 h; the asterisk represents a significant statistical difference at $p < 0.05$) and (b) incubation time versus absorbed protein density.

Apart from this, another study was performed to find out the incubation time, where protein absorption was isolated [Fig. 9(b)]. For this, the experiment was planned with a number of replicates for each composition. All the replicates were divided in a particular set, which was differentiated by the number of hours.

Along with the control disc and sintered HA, all the samples were seeded with a similar concentration of protein for identical timeframes. After every hour, one set of samples was studied for BCA assay. This experiment was performed continuously for a number of hours to determine the isolated stage. For this study (up to 4 h), the protein density increased continuously, but no significant change was observed. After 5 and 6 h of incubation, no changes were observed in the absorbed protein concentration. These experimental results reconfirmed that the absorption mechanism was dependent on the starting protein concentration and material composition.

In closing, it needs to be mentioned that this article possibly provides the first comprehensive report on the mechanical and biological properties of injection-molded HDPE–HA–Al_2O_3 biocomposites. In our earlier work,[24] we found that 30 wt % ceramic filler could only be loaded in the HDPE matrix, and this critical amount was found after systematic analysis of the viscosity and shear flow rate of polymer melts with various ceramic filler additions. No biological study were conducted on the composites in our earlier publication.[24] This research reveals that in the presence of a coupling agent, HDPE with a 40 wt % ceramic loading can be injection-molded without any processing difficulties. The hardness and modulus were higher compared to those reported in our earlier work.[24] On the other hand, a complete *in vitro* biocompatibility study, including cell viability and protein absorption behavior, was performed in this case. With all the mechanical and *in vitro* cytocompatibility results taken together, the injection-molded HDPE composites are considered suitable for preclinical trials and *in vivo* implantation.

CONCLUSIONS

1. This study demonstrated that large square disc (80×80 mm^2) HDPE composites with 40 wt % ceramic filler (HA and/or Al_2O_3) with good mechanical and biocompatibility properties could be obtained with the injection-molding route without any processing difficulties.
2. The Vickers hardness increased with ceramic loading and reached a maximum of about 800 MPa with simultaneous addition of both HA and Al_2O_3 (1 : 1) to 60 wt % HDPE. The tensile test results revealed that a maximum tensile strength of more than 18 MPa and a tensile modulus of close to 855 MPa were achievable with the HDPE composite loaded with 40% ceramic. In addition, a higher compressive strength of 95.6 MPa was measured in the HDPE–20 wt % HA–20 wt % Al_2O_3 composite. Another observation was that the elongation at break decreased with ceramic loading. Interestingly, uniformly distributed HA and Al_2O_3 particles were found to be attached with the deformed polymer matrix on the fractured surfaces.
3. The injection-molded HDPE–HA–Al_2O_3 composites supported the attachment and growth of human osteoblast like SaOS2 cells. The experimental results reveal that the cells were flattened and polygonally shaped, and the spreading/morphological features gave the similitude of cellular junctions.
4. The cell viability of the SaOS2 osteoblast-like cells increased with incubation period (from day 3 to day 7) on the injection-molded HDPE biocomposites, and importantly, a statistically significant difference in terms of cell viability was measured between the injection-molded HDPE–HA–Al_2O_3 and sintered HA.
5. The cell viability results corroborated well with the protein absorption behavior. Protein absorption studies revealed that the absorbed protein density on HDPE–20 wt % HA–20 wt % Al_2O_3 was maximum. In all the composites, the density of the absorbed protein increased with incubation period up to 4 h, which afterward attained a steady state. Similar behavior in terms of cell viability, proliferation, and protein absorption were observed with HDPE–40 wt % HA and HDPE–20 wt % HA–20 wt % Al_2O_3.

The authors thank Department of Biotechnology (DBT), New Delhi, INDIA for the financial support to establish the cell culture facility.

References

1. Weiner, S.; Wagner, H. D. Ann Rev Mater Sci 1998, 28, 271.
2. Martin, R. B.; Burr, D. B. Structure, Function and Adaptation of Compact Bone; Raven: New York, 1989.
3. Ravaglioli, A.; Krawjewski, A.; Celloti, G. C.; Piancastelli, A.; Bachinni, B.; Montanari, L.; Zama, L. Biomaterials 1996, 17, 617.
4. Evans, G. P.; Behiri, J. C.; Bonfield, W.; Currey, J. D. J Mater Sci Mater Med 1990, 1, 38.
5. Goldstein, S. A. J Biomech 1987, 20, 1055.
6. Evans, S. L.; Gregson, P. J. Biomaterials 1988, 19, 1329.
7. Pramanik, S.; Agarwal, A. K.; Rai, K. N.; Garg, A. Ceram Int 2007, 33, 419.
8. Bonfield, W.; Grynpas, M. D.; Tully, A. E.; Bowman, J.; Abram, J. Biomaterials 1981, 2, 185.

9. Bonfield, W. J Biomed Eng 1988, 10, 522.
10. Huang, J.; Di Silvio, L.; Wang, M.; Tanner, K. E.; Bonfield, W. J Mater Sci Mater Med 1997, 8, 775.
11. Huang, J.; Di Silvio, L.; Wang, M.; Rehman, I.; Ohtsuki, I. C.; Bonfield, W. J Mater Sci Mater Med 1997, 8, 808.
12. Suwanprateeb, J.; Tanner, K. E.; Turner, S.; Bonfield, W. J Mater Sci Mater Med 1997, 8, 469.
13. Guild, F. J.; Bonfield, W. Biomaterials 1993, 13, 985.
14. Ward, I. M.; Bonfield, W.; Ladizesky, N. H. Polym Int 1997, 43, 333.
15. Ladizesky, N. H.; Pirhonen, E. M.; Appleyard, D. B.; Ward, I. M.; Bonfield, W. Compos Sci Technol 1998, 58, 419.
16. Reis, R. L.; Cunha, A. M.; Oliveira, M. J.; Campos, A. R.; Bevis, M. J Mater Res Innovat 2001, 4, 263.
17. Pandey, A.; Jan, E.; Aswath, P. B. J Mater Sci 2006, 41, 3369.
18. Joseph, R. Ph.D. Thesis, University of London, 2001.
19. Wang, M.; Joseph, R.; Bonfield, W. Biomaterials 1998, 19, 2357.
20. Ton That, P. T.; Tanner, K. E.; Bonfield, W. J Biomed Mater Res 2000, 51, 461.
21. Wang, M.; Bonfield, W. Biomaterials 2001, 22, 1311.
22. Wang, M.; Porter, D.; Bonfield, W. Br Ceram Trans 1994, 93, 91.
23. Nath, S.; Bodhak, S.; Basu, B. J Biomed Mater Res Part B: Appl Biomater 2009, 88, 1.
24. Basu, B.; Jain, D.; Kumar, N.; Choudhury, P.; Bose, A.; Bose, S.; Bose, P. J Appl Polym Sci 2011, 121, 2500.
25. Tripathi, G.; Dubey, A.; Basu, B. J Appl Polym Sci, Article in press(corrected Proof).
26. Bodhak, S.; Nath, S.; Basu, B. J Biomater Appl 2009, 23, 407.
27. Xavier, S. F.; Schultz, J. M.; Friedrich, K. J Mater Sci 1990, 25, 2428.
28. Nath, S.; Dey, A.; Mukhopadhyay, A. K.; Basu, B. Mater Sci Eng 2009, 513–514, 197.
29. Sousa, R. A.; Reis, R. L.; Cunha, A. M.; Bevis, M. J. J Appl Polym Sci 2003, 89, 2079.
30. Sadi, A. Y.; Homaeigohar, S. S.; Khavandi, A. R.; Javadpour, J, J Mater Sci Mater Med 2004, 15, 853.
31. Sousa, R. A.; Reis, R. L.; Cunha, A. M.; Bevis, M. J. Compos Sci Tech 2003, 63, 389.
32. Carmen, A.; Rosestela, P.; Arquimedes, K.; Gema, G.; Nohemy, D.; Yanixia, S.; Luís, B. J. Macromol Symp 2007, 247, 190.
33. Parra, C.; Gonzalez, G.; Albano, C. Macromol Symp 2009, 286, 60.
34. Deligianni, D. D.; Katsala, N. D.; Koutsoukos, P. G.; Missirlis, Y. F. Biomaterials 2001, 22, 87.
35. Puleo, D. A.; Holleran, L. A.; Doremus, R. H.; Bizios, R. J Biomed Mater Res 1991, 25, 711.
36. Hott, M.; Noel, B.; Bernache-Assolant, D.; Rey, C.; Marie, P. J. J Biomed Mater Res 1997, 37, 508.
37. Zreiqat, H.; Evans, P.; Rolfe Howlett, C. J Biomed Mater Res 1999, 44, 389.
38. Wang, D.; Douma, M.; Oleschuk, R. D.; Horton, J. H. J Colloid Interface Sci 2009, 331, 90.